ELSEVIER

Ca²⁺ vs. Ba²⁺ electrochemical detection by two disubstituted ferrocenyl chalcone chemosensors. Study of the ligand–metal interactions in CH₃CN

Béatrice Delavaux-Nicot [a,*], Jérôme Maynadié [a], Dominique Lavabre [b],
Suzanne Fery-Forgues [b]

[a] *CNRS: National Center of Scientific Research, Laboratoire de Chimie de Coordination du CNRS, UPR 8241,
205, route de Narbonne, F-31077 Toulouse cedex 04, France*
[b] *Laboratoire des Interactions Moléculaires et Réactivité Chimique et Photochimique, UMR 5623 du CNRS,
Université Paul Sabatier, F-31062 Toulouse cedex 9, France*

Abstract

We show here that the disubstituted ferrocenyl chalcones **1** and **2** are good electrochemical sensors for calcium and barium in CH₃CN. However, these two triflate salts are detected in a different way by both ligands. To clarify this point, a thorough and informative NMR study of the ligand–salt interactions is presented. The unusual shapes of the titration curves obtained depend on both the ligand and cation used. For example, they illustrate that ligand **1** mainly interacts with the metal by its CO functions, while ligand **2** also interacts by its azacrown groups. These curves also reflect complex equilibriums in solution involving several ligand–salt adducts detected by mass spectrometry. To evaluate the strength of these interactions, the association constants of all the species formed have been determined by fitting the NMR data. It is noteworthy that changing the diethylamino groups in molecule **1** by the azacrown residue enhances the selectivity for the calcium salt, as pointed out by the value of the association constant of the **2**Ca²⁺ species. The synthesis of the protonated counterparts **3** and **4** was useful to clarify the electrochemical behaviour of **1** and **2**. Although the two ligand–salt interactions present several common points, the whole results obtained allow us to propose an original explanation for the difference observed between the Ca²⁺ and Ba²⁺ electrochemical sensing.
© 2006 Elsevier B.V. All rights reserved.

Keywords: Chalcone; Ferrocene; Chemosensors; Ligand–cation interaction; Electrochemical properties

1. Introduction

Ferrocenyl chalcones have regularly been the subject of many interesting papers dealing with varied aspects of their chemistry [1] or potential uses in different fields [2]. As far as we are concerned, we have recently demonstrated their ability in behaving as ion chemosensors. Actually, to get a new generation of original electrochemical and optical ferrocenyl ion chemosensors [3], we have designed a family of ferrocenyl compounds according to a "three-component

conjugated system" concept [3c]. In contrast with reported systems [3d,3e,4], in these compounds the ferrocenyl, complexing, and fluorescent moieties are not connected by a saturated link but belong to the same conjugated electron system. In particular, we have showed that the monosubstituted ferrocenyl derivatives containing the basic fragment (–CO(CH=CH)C₆H₄-*p*–R), where R is an amino alkyl or azacrown group, are good electrochemical [5,6] and optical (UV–vis absorption) [7] calcium sensors, though they are not fluorescent. However, the fact that the corresponding disubstituted compounds [Fe(C₅H₄CO(CH=CH)ₙC₆H₄-*p*-R)₂], $n = 1$, R = NEt₂ (**1**) [8] (Scheme 1), and $n = 2$, R = NMe₂ (**A**) display remarkable fluorescence properties

---

* Corresponding author. Tel.: +33 5 61 33 31 00; fax: +33 5 61 55 30 03.
E-mail address: delavaux@lcc-toulouse.fr (B. Delavaux-Nicot).
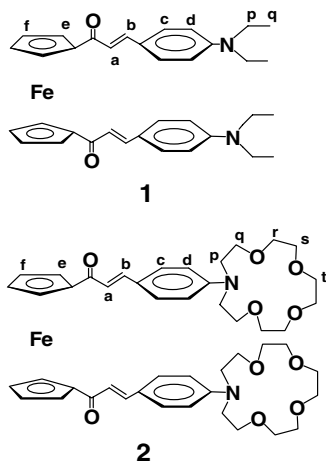
Scheme 1. Compounds **1** and **2**.

in acetonitrile is of particular interest, and we have recently reported the capacity of **A** for behaving as a multiresponsive calcium chemosensor [9].

We are interested in the different factors that could influence the physical properties in this family, and in the processes leading to the detection phenomena. Therefore, in this article, we focus on the capacity of compound **1** for behaving as a cation electrochemical chemosensor. Some preliminary results about this compound have already been published [8]. We compare the behaviour of **1** with that of its disubstituted counterpart [Fe(C$_5$H$_4$COCH=CHC$_6$H$_4$-*p*–aza-15-crown-5)$_2$] (**2**) (Scheme 1), where the diethylamino groups have been replaced by the azacrown residues. The electrochemical response of both compounds in the presence of different cations was investigated. In particular, we show that, in contrast to the monosubstituted derivatives, compound **1** and **2** are in fact clearly electrochemically sensitive to the presence of the Ba^{2+} cation but in a "non-classical way". We describe the synthesis and characterization of the two new protonated compounds [(**1**)2H^{2+}][BF$_4^-$]$_2$ (**3**) and [(**2**)2H^{2+}][BF$_4^-$]$_2$ (**4**) (Scheme 2), which were necessary to clarify the electrochemical behav-

iour in the presence of cations. The interactions that take place between ligands **1**–**2** and the Ca^{2+} and Ba^{2+} cations have been thoroughly investigated by NMR spectroscopy. Thus, we show that each interaction gives rise to a complex equilibrium between several species in solution, and is representative of both the nature of the ligand and that of the cation involved. Interestingly, we give evidence that for both receptors **1** and **2**, the Ca^{2+} and the Ba^{2+} electrochemical detection processes are different in nature.
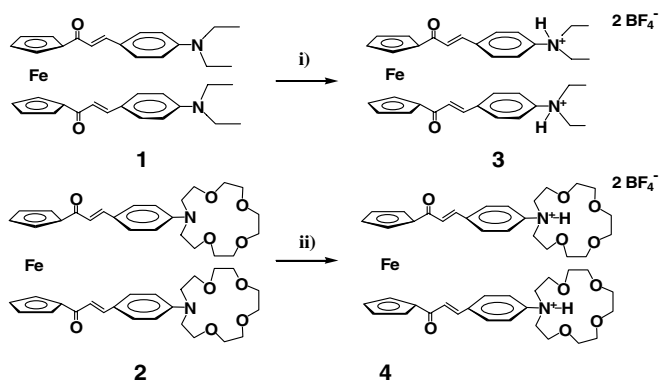
2. Results and discussion

2.1. Synthesis and characterization of compounds 1–4

Compounds **1** and **2** were obtained by reaction of [Fe(C$_5$H$_4$COMe)$_2$] with *p*-dimethylaminobenzaldehyde, and with crown aldehyde [*N*-(4-formylphenyl)aza-15-crown-5] respectively, in basic aqueous solution [3c]. Our newly published procedure [5] used for the synthesis of the monosubstituted ferrocenyl chalcones was successfully applied to the synthesis of the disubstituted compounds **1**–**2**. It allows the facile isolation of compound **2** and a significant improvement (from 7% to 60%) on the isolated yield of **1** when compared to our original procedure. ^{1}H and ^{13}C 2D NMR characterization was undertaken in CD$_3$CN (see Section 4). It provides a good assignment of each signal necessary to compare **1** and **2** with their protonated derivatives, and to monitor their interaction with salts by NMR spectroscopy. In comparison with **1**, which has nearly the same signals in this solvent, the CH$_2$ crown signals situated in the δ = 3.5–3.8 ppm range appear as the ^{1}H NMR signature of the compound (see Fig. 1). The values of the Hp–t chemical shifts are close to those reported for other crown compounds [6,10]. The NMR spectra reveal the symmetry of the molecule in solution, and confirm that the structure is close to that of its X-ray characterized monosubstituted counterpart [(C$_5$H$_5$)Fe(C$_5$H$_4$-COCH=CHC$_6$H$_4$-*p*–aza15-crown-5)] but with a second organic arm.

We will see in Section 2.4. that comparing the ligands with their protonated derivatives proved to be useful to clarify the electrochemical behaviour. Consequently, the protonated derivatives of compounds **1** and **2** were prepared here. Treatment of a CH$_3$CN solution of compound **2** with HBF$_4$ · Et$_2$O in a 1/2 stoichiometry turned the mixture from orange to pink and afforded the protonated species [(**2**)2H^{2+}][BF$_4^-$]$_2$ (**4**, Scheme 2). This new compound was isolated as a violet powder in a 65% yield. As described in the Experimental Section, elemental analyses and mass spectra are in agreement with the proposed formula for **4**, and the characterization of this compound was fully achieved by ^{1}H and ^{13}C 2D NMR measurements. The signal situated at δ = 8.52 ppm is attributed to the protons of the NH$^+$ groups. The protonation of the nitrogen atom affects the whole molecule **2** as illustrated by Table 1. In particular, when compared to **2**, the most significant downfield-shifted chemical shift variations are observed for the

Scheme 2. Synthetic route for compounds **3** and **4**. Reagents and conditions: (i) Et$_4$NBF$_4$ 2 equiv, Ca(CF$_3$SO$_3$)$_2$ 2 equiv, CD$_3$CN, 4 h, 20 °C. (ii) HBF$_4$ · Et$_2$O 2 equiv, CH$_3$CN, 20 °C.
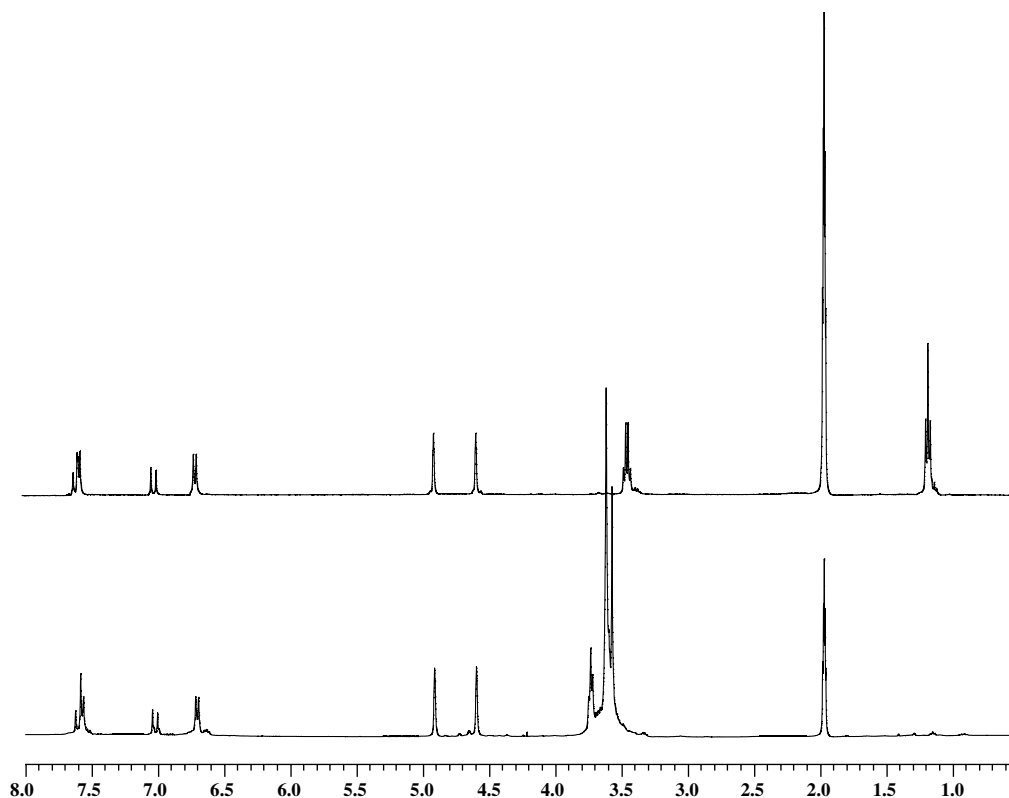
Fig. 1. ^{1}H NMR spectra of compounds **1** (top) and **2** (bottom) (400 MHz, CD$_3$CN, 293 K), in the $\delta = 0.5$–8 ppm range.

Hc, Hd, and Hp protons. The HMQC measurements indicated that the Hq and Hr protons of the crown groups are diastereotopic.

The latter synthetic protonation route did not lead to clear characterization of compound $[(\mathbf{1})2\mathrm{H}^{2+}][\mathrm{BF}_4^-]_2$ (**3**) starting from **1**. Actually, under these conditions, rapid formation of by-products also prevented its successful isolation. However, in the mixture formed, compound **3** was detected by the presence of its $[\mathrm{M}-\mathrm{BF}_4]^+ = 677$ peak in the MS (FAB) spectrum. In the light of the outcome of previous study about the reactivity of the monosubstituted compounds of this family, the synthesis of compound **3** was then performed by subsequently reacting compound **1** with 2 equiv of NEt$_4$BF$_4$ and 2 equiv of Ca(CF$_3$SO$_3$)$_2$ in CD$_3$CN. After 4 h, compound **3** was the only product obtained in solution and its characterization was achieved

by NMR (see Section 4). As shown by Fig. 2, we note that the signal attributed to the CH$_2$ protons appears now as a complex multiplet and that the NH$^+$ signal is situated at 9.14 ppm. Table 1 indicates that, as for **2**, the Hc, Hd, and Hp protons are strongly perturbed by the protonation reaction. Moreover mass spectrometry measurements (FAB > 0) performed on this mixture revealed the peak expected for the $[\mathbf{3}\text{-}\mathrm{CF}_3\mathrm{SO}_3]^+$ species. Unfortunately, it was not possible to properly isolate the product.

2.2. Electrochemical study

2.2.1. Characterization of ligands 1–2

The electrochemical properties of compounds **1** and **2** have been investigated in CH$_3$CN. For comparison purpose, the solutions were light-protected, as it was also the

Table 1
Selected NMR chemical shift variations ($\Delta\delta$ in ppm) induced by protonation of compounds **1** and **2** to give compounds **3** and **4**, respectively; $L = 5 \times 10^{-3}$ M, CD$_3$CN at 293 K

	CHa	CHb	CHc	CHd	CHe	CHf	CHp	CHq	CHr	CO
$\delta(\mathbf{3})$–$\delta(\mathbf{1})$										
^{1}H	0.29	0.12	0.44	0.92	0.11	0.15	0.23	–	–	–
^{13}C	8.42	−3.51	−0.20	11.79	0.48	1.02	10.12	–	–	−0.06
$\delta(\mathbf{4})$–$\delta(\mathbf{2})$										
^{1}H	0.32	0.14	0.47	1.25	0.10	0.14	0.34	[a]	[a]	–
^{13}C	7.93	−3.23	−0.22	12.34	0.41	1.03	5.90	−5.33	0.36	−0.04

[a] Diastereoisotopic groups.
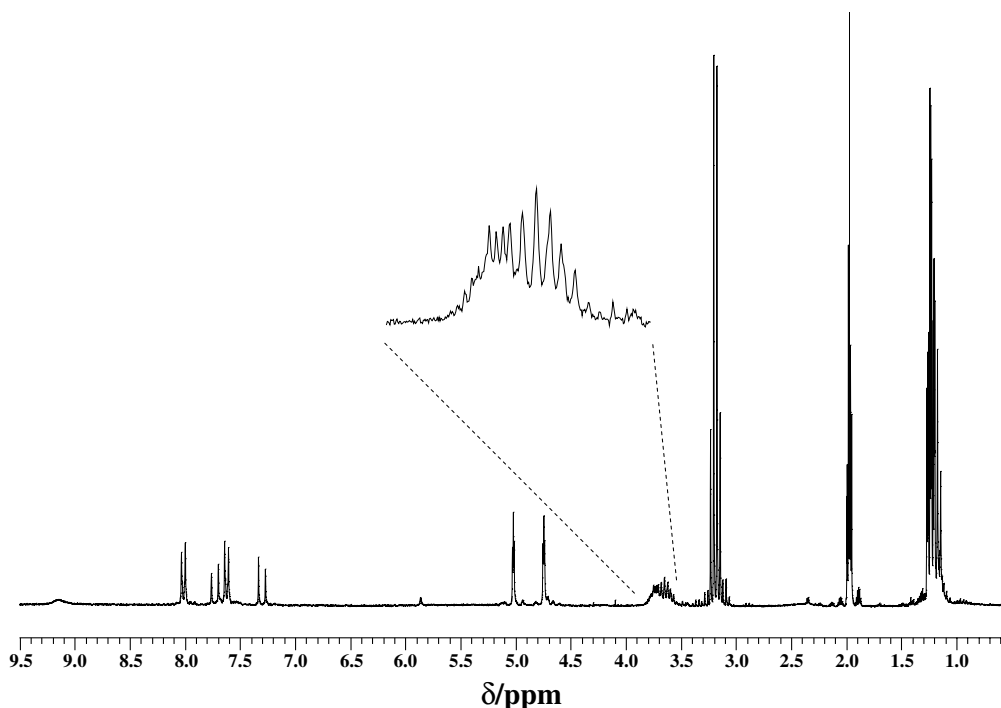
Fig. 2. ^{1}H NMR spectrum (250 MHz, CD$_3$CN, 293 K), in the $\delta = 0.5$–9.5 ppm range of a mixture of **1** + 2 equiv of Ca(CF$_3$SO$_3$)$_2$ and 2 equiv of Et$_4$NBF$_4$ after 4 h. These conditions lead to the formation of compound **3**.

case for their protonated derivatives that are sensitive to light. A typical cyclic voltammogram (CV) of compound **2** is shown in Fig. 3. It reveals that the electrochemical characteristics of **2** are similar to those of compound **1**. This electrochemical trend has also been observed for related compounds, where the alkyl groups have been replaced by crown groups [6,11a]. In oxidation, the first wave observed corresponds to an irreversible and complex oxidation process of compound **2**. It may be attributed to the oxidation of the organic amine moiety [6,7,9,11] whose first oxidation potential $E_{1/2}$Org is 0.81 V. The wave observed at Ep$_a$ ≅ 1.12 V is due to the oxidation of the fer-rocene moiety and corresponds to a quasi-reversible

Fig. 3. Cyclic voltammograms of compounds **1** (dashed line) and **2** (solid line). Experimental conditions: Pt electrode (1 mm diameter) in 0.1 M solution of ^{n}Bu$_4$NBF$_4$ in CH$_3$CN, scan rate 100 mV s^{-1}, ligand concentration 10^{-3} M; reference electrode SCE.

process ($E_{1/2} = 1.05$ V). In reduction, the single wave observed Ep$_a = -1.76$ V is attributed to a reduction process mainly located on the CO function.

The main difference between the CV of **1** and **2** is the fact that the organic moiety of compound **2** is slightly more difficult to oxidize than that of **1**. Actually, for **2**, an anodic shift of 70 mV of the first oxidation potential of the organic moiety is observed when compared to that of **1**. This is due to the presence of the electron-withdrawing oxygen atom which decreases the donor strength of the nitrogen atom [6].

It is noteworthy that substituting a cyclopentadienyl proton of the monosubstituted compounds [(C$_5$H$_5$)Fe-(C$_5$H$_4$COCH=CHC$_6$H$_4$NEt$_2$)] (**5**) [5] and [(C$_5$H$_5$)Fe(C$_5$H$_4$-COCH=CHC$_6$H$_4$-p–aza15-crown-5)] (**6**) [6] by a second organic aza arm to give the corresponding compounds **1** and **2** induces a remarkable change in the electrochemical properties. Actually, in both monosubstituted compounds **5** and **6**, the ferrocene moiety is clearly responsible for the first oxidation process and the organic aza moiety for the following processes. It is the opposite in both disubstituted compounds **1** and **2**: the oxidation of the organic link precedes the oxidation of the ferrocene moiety. However, the explanation of this "inversion of potential" is not obvious since this behaviour is not systematic. For example, for both the monosubstituted compound [(C$_5$H$_5$)Fe(C$_5$H$_4$-COCH=CHC$_6$H$_4$NMe$_2$)] (**7**) [5] and its disubstituted homologue [Fe(C$_5$H$_4$CO(CH=CH)$_2$C$_6$H$_4$-p–NMe$_2$)$_2$] (**A**) [9] the first oxidation potential is that of the organic moiety(ies). A series of theoretical calculations are underway to understand this intriguing behaviour.

2.2.2. Electrochemical cation detection study

To investigate the cations detection properties of compounds **1** and **2**, electrochemical tests were performed in acetonitrile in the presence of Na^+, Zn^{2+}, Ca^{2+}, Mg^{2+}, and Ba^{2+} triflates. During these new experiments, equivalent of salts were added until a clear reproducible and final shift was observed in each case. Some common trends appeared. In particular, we noted that both compounds were not sensitive to the presence of the Na^+ cation, and hardly sensitive to the presence of Zn^{2+}. However, they were sensitive to the presence of the Ca^{2+} and Mg^{2+} cations. We were especially interested by these cations for comparison purpose with other ligands of this chalcone family. In this case, a cathodic shift of around -120 mV of the oxidation potential of the Fe^{II}/Fe^{III} couple is observed upon addition of two [8], and 4 equiv of salt respectively (see Table 2). In addition, the disappearance of the wave corresponding to the first oxidation process of the organic moieties and the marked broadness and evolution of the reduction process were clearly observed, indicating that the whole conjugated organic parts of the molecule were also strongly affected [8]. In reduction, a new irreversible process appeared around $Ep_a = -340$ mV for **1** and -280 mV for **2**, respectively. These latter phenomena are faster and more clearly observed for the Ca^{2+} salt.

Interestingly, upon Ba^{2+} addition (6 and 4 equiv for **1** and **2**, respectively), for both compounds the electrochemical detection is different: an anodic shift of the first oxidation potential of the organic moiety, 130 and 30 mV, respectively, is observed whereas the oxidation potential of the ferrocene moiety remains nearly the same. Fig. 4 is provided as a chosen illustration for the (Ba^{2+}, **1**) couple in oxidation. The reduction process is strongly perturbed here with a broad ill-defined wave situated around $Ep_a = -1200$ mV. The potential of the latter wave increases with salt concentration. Fig. 5 also illustrates the different behaviour of **2** depending on the nature of the salt used. In the case of compound **1**, it is noteworthy that an anodic shift of the Ep_a of the organic moiety (50 mV) and of the ferrocene moiety (20 mV) are observed for the zinc cation (6 equiv), however the $\Delta E_{1/2}$ values remain nearly the same.

Table 2
Selected electrochemical characteristics of compounds **1** and **2** upon addition of the indicated number of salt equivalents

Salt	Eq.	$\Delta E_{1/2}$ Fe	$\Delta E_{1/2}$ Org
Compound **1**			
Ba^{2+}	6	0	120
Ca^{2+}	2	-130	–
Mg^{2+}	4	-110	–
Compound **2**			
Ba^{2+}	4	0	30
Ca^{2+}	2	-120	–
Mg^{2+}	4	-120	–

$\Delta E_{1/2}$ (mV), Org = first oxidation process of the organic part of the molecule; ligand concentration 10^{-3} M.
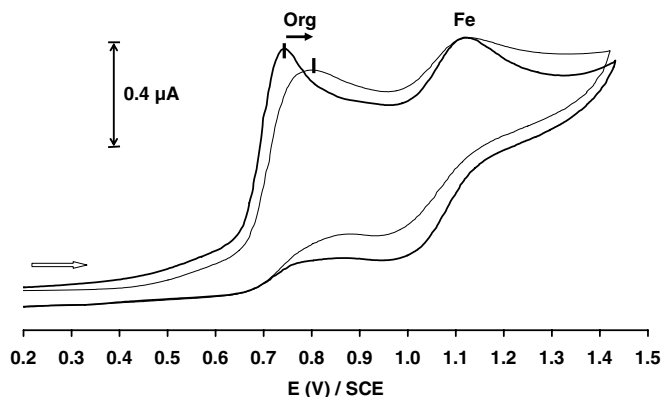
Fig. 4. Cyclic voltammograms of compound **1** in oxidation (bold line) and **1** + 2 equiv of $Ba(CF_3SO_3)_2$ (solid line). Experimental conditions: Pt electrode (1 mm diameter) in 0.1 M solution of $^nBu_4NBF_4$ in CH_3CN, scan rate 100 mV s^{-1}, ligand concentration 10^{-3} M; reference electrode SCE.
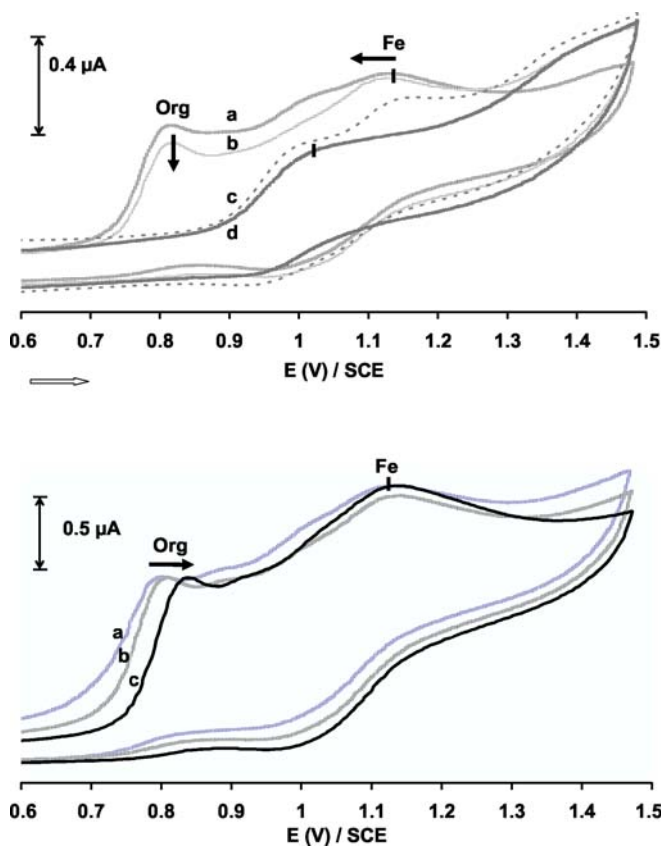
Fig. 5. Top: from top to bottom: cyclic voltammograms of (a) **2**, (b) **2** + 1 equiv $Ca(CF_3SO_3)_2$, (c) **2** + 2 equiv $Ca(CF_3SO_3)_2$, and (d) after 10 min. Bottom: cyclic voltammograms of (a) **2**, (b) **2** + 1 equiv $Ba(CF_3SO_3)_2$, and (c) **2** + 4 equiv $Ba(CF_3SO_3)_2$. Experimental conditions: Pt electrode (1 mm diameter) in 0.1 M solution of $^nBu_4NBF_4$ in CH_3CN, scan rate 100 mV s^{-1}, ligand concentration 10^{-3} M; reference electrode SCE.

Generally, cation detection by ferrocene derivatives is mainly based on the variation of the oxidation potential of the ferrocene unit [12], and the variations associated with other oxidation or reduction processes are rarely con-

sidered or explained. In the present cases, the observation that the barium electrochemical detection did not induce the same perturbations of the oxidation process as the calcium salt (or magnesium salt) prompted us to get a deeper insight into this phenomenon. In the light of our knowledge about this family of compounds, the link between cation interaction and cation electrochemical detection was investigated for ligands **1** and **2** with both the Ca^{2+} and Ba^{2+} salts. This is the reason why the NMR study concerning the different ligand–cation interactions is presented below.

2.3. NMR and mass spectrometry investigations of the ligand–cation interactions

2.3.1. Focus on the Ca^{2+} Cation

The NMR experiments were performed at 293 K, using first 2 equiv of salts in CD_3CN (see Section 4).

As previously reported for compound **1** [8], 2 D NMR analyses highlighted that the CHb and CO groups are characteristic sites indicating a CO-salt interaction and an influential role of the double bond. Actually, these groups display the most important ^{13}C shift variations. This fact is confirmed by the ^1H NMR spectrum (see Table 3) showing that the strongest downfield shift occurs for the Hb protons. The NEt_2 groups are the only groups not to be affected by this interaction. These trends are reminiscent of those observed for the monosubstituted homologue **5** under the same conditions. In the case of compound **2**, the Hd protons are strongly deshielded, clearly indicating an interaction with the azacrown groups. However, the Hb protons of **2** are also significantly perturbed. The latter observation reveals that a competitive CO interaction occurs for **2**, which is in line with our previous ^{13}C NMR study on the monosubstituted analogue **6** [6].

The ^1H NMR behaviour of compounds **1** and **2** was further examined in the presence of calcium salt by varying the calcium concentration in order to get a better insight into the L–Ca^{2+} interaction processes. In both cases, the continuous shifts of the sharp peaks observed during the calcium titration experiments were indicative of the presence of fast equilibriums on the NMR time scale [13]. By chance, the chemical shift variations of five protons of **1** and of 6 protons of **2** could be successfully monitored and were plotted vs. calcium concentration (Fig. 6, top, points). For both

compounds, the chemical shift variations on most of the Ha–f protons confirm that the whole unsaturated core of the molecule including the Cp rings contributes to the electronic interaction with calcium. In the case of **2**, the azacrown ring is also clearly involved as shown by the Hp protons shift variation. The non-classical shapes of the curves obtained (especially for **2**) are in agreement with the involvement of multiple equilibriums in solution. A remarkable fact is the ability of the Ha–c protons of **1**, and Ha–d protons of **2** to undergo different chemical shift variations (downfield or upfield shift variations) according to the salt concentration.

Processing the NMR data acquired can provide the number and stoichiometry of the calcium adducts in the L–Ca^{2+} interactions. The curves obtained by plotting the chemical shift variation vs. calcium concentration were processed according to a global curve-fitting method previously reported [5,9,14], and the analysis was performed simultaneously for the five and six protons of **1** and **2** respectively. In Fig. 6 top, we display the ^1H NMR experimental data points together with the calculated curves to show the quality of the fit. Complete agreement between theory and experiment could only be obtained by taking into account the existence of four and five L_nM_m species of different stoichiometries for compounds **1** and **2** respectively. These L_nM_m species are formed by interaction of the ferrocenyl ligand L (**1**, **2**) with the calcium cation M. Their corresponding association constants (K_n) are given in Table 4.

As shown by Fig. 6 (bottom), the profile of the curve obtained by calculating the concentrations of the species formed vs. calcium concentration is quite different for **1** and **2**. This is directly related to the nature of the ligand (*N*-alkyl or *N*-crown), and consequently to the nature and number of the main interacting sites (CO or both crown and CO). Regarding compound **1**, the substoichiometric species are the main species at low concentration, and the concentration of the $1M_2$ species increases rapidly until this compound becomes the major species at high concentration. The 1_2M species displays the highest association constant. For compound **2**, the concentration of the 2_2M and 2_3M species rapidly decreases. The main characteristic feature is the specific formation of the **2M** species around 1 equiv of calcium, giving rise to a "bell" curve. Contrary to compound **1**, a fifth LM_3 ($2M_3$) species can be formed, probably by interaction of both the CO and two crowns groups of the same molecule with three different calcium cations. The association constant corresponding to the $2M_3$ species is the lowest of all. This low value is probably due to repulsive electrostatic effect between three neighbouring cations.

Let us come back to the **2M** species. It is striking to see that this species exhibits the highest association constant in this family of compounds (2.35×10^5 L mol^{-1}). This can be explained by the fact that the crown ring fits well the calcium ion [15]. Besides, when compared to its monosubstituted counterpart **6**, the presence of the second crown

Table 3
^{13}C NMR CO chemical shift variation and selected ^1H NMR shift variations ($\Delta\delta$, ppm) of the indicated groups for compounds **1–2** and compounds **5–6** upon addition of 2 equiv, and 1 equiv of calcium salt, respectively[a]

Compound	Ha	Hb	Hc	Hd	Hp	He	Hf	CO
1	−0.08	0.32	−0.09	−0.11	−0.03	0.16	0.21	3.26
5	−0.01	0.17	0.01	−0.02	−0.00	0.11	0.09	2.77
2	0.06	0.12	0.13	0.46	−0.05	0.08	0.14	1.25
6	0.11	−0.02	0.15	0.59	−0.15	0.06	0.11	1.48

[a] [L] = 5×10^{-3} M; see group labelling in Scheme 2.

Compound **1**   Compound **2**
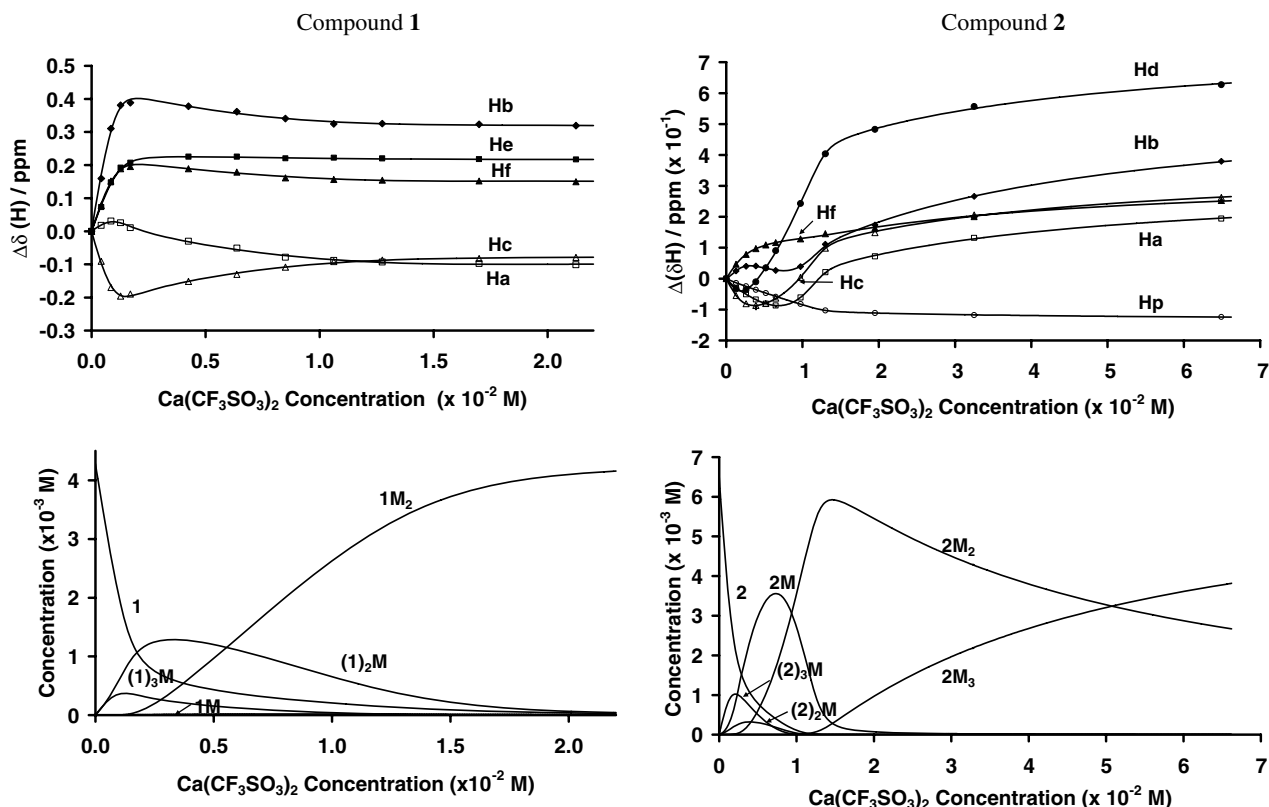
Fig. 6. Top: ^{1}H NMR chemical shift variations of the mentioned protons of **1** (5.0×10^{-3} M) (left), and **2** (6.5×10^{-3} M) (right) vs. $Ca(CF_3SO_3)_2$ concentration in CD_3CN at 293 K. Experimental values (dots) and calculated curves (lines) obtained by fitting the data. See atom labelling in Scheme 1. Bottom: concentration of the formed species with **1** (left) and with **2** (right) vs. the $Ca(CF_3SO_3)_2$ concentration.

Table 4
Association constants (K_n in L mol^{-1}) related to the different species formed with ligand **1** or **2** and calcium triflate in acetonitrile, determined by processing the NMR data (values given with ±15% error)

Compound	Salt	LM K_1	L$_2$M K_2	LM$_2$ K_3	L$_3$M K_4	LM$_3$ K_5
1	Ca^{2+}	2.22×10^1	1.66×10^5	3.21×10^4	2.93×10^2	–
2	Ca^{2+}	2.37×10^5	1.29×10^2	1.27×10^4	2.12×10^3	2.89×10^1
1	Ba^{2+}	8.92×10^1	1.01×10^3	2.58×10^2	2.43×10^3	2.60×10^1
2	Ba^{2+}	1.94×10^3	2.29×10^1	2.96×10^2	5.38×10^3	–

arm in **2** enhances the value of the association constant of the **2M** species by two orders of magnitude. This **2Ca^{2+}** species is probably formed by a Ca^{2+} cation sandwiched between two crown rings of the ligand [16]. In the literature, although numerous calcium-containing structures are known, only a few azacrown calcium complex X-ray structures have been reported for azacrown complexes [17], and unfortunately, it was not possible to obtain any X-ray structures for this **2M** species.

This NMR analysis has shown that the same interacting sites are involved for ligands **1** and **5**, and for ligands **2** and **6**, respectively, as long as their interaction with the Ca^{2+} salt is considered. However, if comparing the monosubstituted compounds with the disubstituted counterparts it appears that a second organic arm in the molecule increases the number of species involved in the equilibrium

processes and the number of possible associations for a species formed and a given stoichiometry. Actually, as previously developed [5,6], several species could be envisaged for a specific L$_n$M$_m$ stoichiometry. Several factors have to be taken into account, as for example the number of arms of the molecules or the number of coordinating sites involved in the formation of the adducts. The coordinating solvent molecules and the different donor atoms of the CF$_3$SO$_3$ anion may also interfere [18]. It is noteworthy that, in these equilibriums, weak intermolecular or electrostatic interactions may also be considered rather than classical complexation reactions [19].

Thus, for the concentrations used, several species compete in solution. To provide strong support for their formation in solution, samples of **1** and **2** (5×10^{-3} M) containing 0.5, 1, and 2 equiv of calcium salt were prepared as for

Table 5
Assignment of the main peaks obtained by mass spectrometry using the positive FAB and the ESI-MS techniques for compounds **1** and **2** ($L = 5 \times 10^{-3}$ M) in the presence of calcium

Compound	Salt	$[LMX]^+$	$[L_2MX]^+$	$[L_3M]^{2+}$	$[LM_2X_3]^+$	$[LM_3X_5]^+$
1	Ca^{2+}	777	1366	903	1115	–
2	Ca^{2+}	1069	1951	1341	1407	1745
1	Ba^{2+}	875	1463	952	1311	1746
2	Ba^{2+}	1167	2048	1391	1603	–

NMR measurements, and their mass spectra were recorded using the positive FAB technique with an MNBA matrix as well as the ESI-MS technique. All the peaks expected for the different compounds were effectively detected (see Table 5).

2.3.2. Focus on the Ba^{2+} Cation

During the titration experiments of compound **1** with Ba^{2+}, the solution turned from orange to red. The chemical shift variations of six protons were successfully plotted vs. barium concentration (Fig. 7 top, left). From a general point of view, the curves are flatter than those obtained with the calcium salt and **1**. This is in agreement with the fact that the barium cation has a lower charge density than the calcium cation [20], thus inducing a lower chemical shift variation for a given salt concentration. A neat difference is observed for the Ha protons that depict here a monotonous

shift variation contrary to their behaviour with the calcium salt. However, when comparing with the calcium interaction, the general trends remain the same, and consequently a CO-centered interaction can also be proposed for Ba^{2+}.

Regarding compound **2**, its NMR behaviour with the barium salt is quite close to that observed with the calcium salt. The same trends are observed for the Ha, Hc, Hd, Hp protons. A difference is noted for the Hb protons, whose "two-wave" behaviour visible in Fig. 6 top disappears, and whose chemical shift variation magnitude was weaker when replacing calcium by barium. The crown protons Hp and Hr undergo a strong variation of their chemical shift. This confirms that the interaction with barium involves the whole conjugated electron system and the crown group.

These new data were processed with the curve-fitting model. For compound **1**, in addition to the species already encountered in the interaction with the calcium, the new
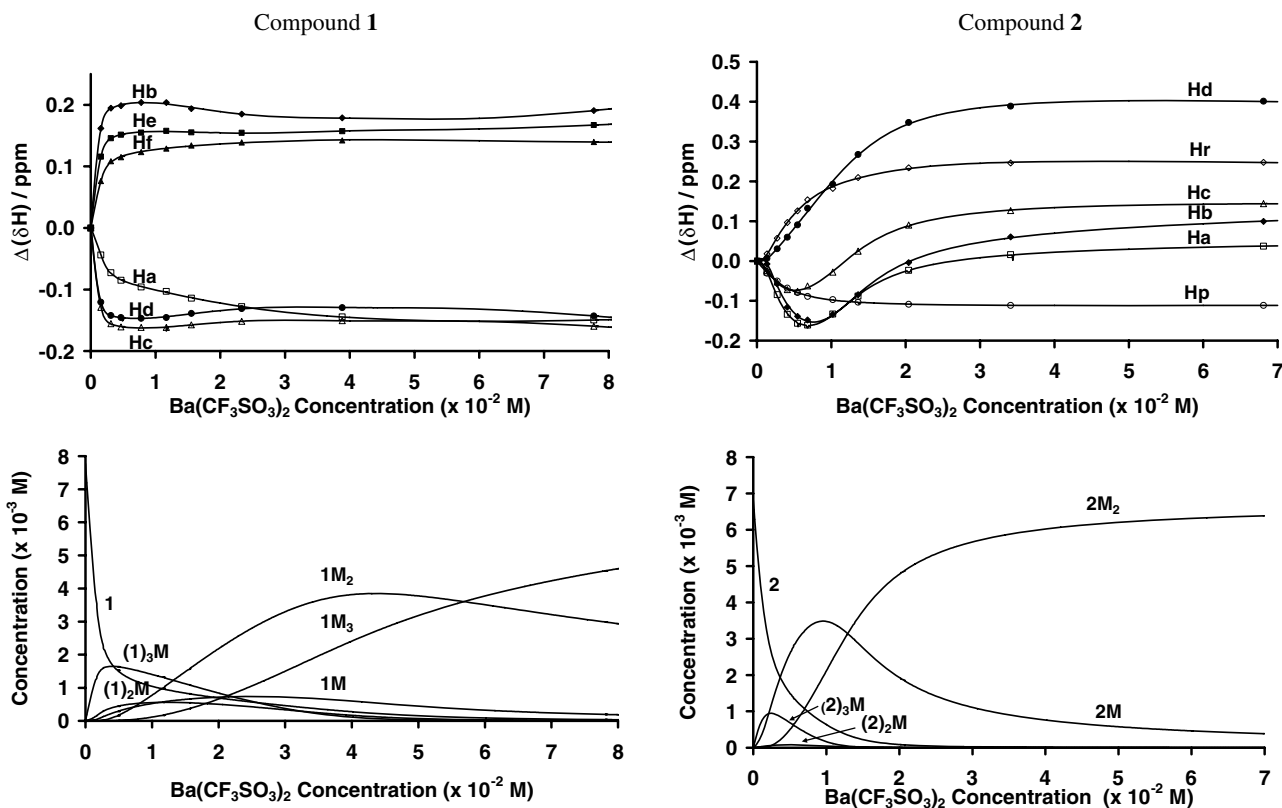
Fig. 7. Top: ^{1}H NMR chemical shift variations of the mentioned protons of **1** (7.8×10^{-3} M) (left), and **2** (6.8×10^{-3} M) (right) vs. Ba(CF$_3$SO$_3$)$_2$ concentration in CD$_3$CN at 293 K. Experimental values (dots) and calculated curves (lines) obtained by fitting the data. See atom labelling in Scheme 1. Bottom: concentration of the species formed with **1** (left), and with **2** (right) vs. Ca(CF$_3$SO$_3$)$_2$ concentration.

species $1M_3$ is required to have a good fit. This species displays the lowest association constant with Ba^{2+}, whereas the substoichiometric 1_2M and 1_3M species have the highest ones, as for the calcium salt.

For compound **2**, the different L_nM_m species formed appear in the same order as those formed with the calcium salt. However, the bell curve of the **2M** complex is flattened, and this species finally competes with the $2M_2$ species at high salt concentration. The $2M_3$ species does not exist, probably because of both steric hindrance, and electrostatic repulsion. It is noteworthy that the bis-crown compound **2** is better suited for the complexation of calcium than for that of the bulky barium cation, as reflected by the respective association constant of the LM species.

From a general point of view, the association constants of the species formed with the Ba^{2+} cation are weaker than with the Ca^{2+} cation. For both ligands **1** and **2**, the highest Ba^{2+} association constant is obtained for the L_3M species. This could be explained by the propensity of the Ba^{2+} cation to promote intermolecular interactions [21].

As for calcium, mass spectrometry measurements performed on ligands **1**–**2** with the barium salt and under the same experimental conditions support the existence of the different species in solution (see Table 5).

2.4. Link between cation interaction and cation electrochemical detection by ligands 1 and 2

The NMR study has shown that, for each disubstituted ligand, changing the Ca^{2+} salt by the Ba^{2+} salt induces some differences but the interacting sites remain the same. Therefore, at this point the paramount question is: why is the Ca^{2+} electrochemical detection so different from that of Ba^{2+}?

In previous papers, we have established for the monosubstituted compounds **5**, **6** and for compound **A**, that the Ca^{2+} electrochemical detection is the result of a two-step process under our electrochemical conditions. Actually, a complex Ca^{2+} interaction with the ligand promotes a subsequent protonation reaction in presence of the $^nBu_4NBF_4$ salt and water traces. This protonation reaction is responsible for the Ca^{2+} electrochemical detection that induces a potential shift of the Fe^{II}/Fe^{III} couple and the disappearance of the waves corresponding to the oxidation processes of the organic arms of the molecules. The new wave observed in reduction corresponds to the NH^+ reduction process.

These electrochemical changes are close to those observed with compounds **1** and **2** in Section 2.2.2. It has also been verified that the CV of ligand **1** and **2** upon addition of 2 equiv of calcium is quite similar to those of **1** and **2** upon 2 equiv of acid, respectively. Moreover, we have shown in Section 2.1 that it is possible to synthesize protonated compound **3** by reacting **1** with appropriate amounts of $Ca(CF_3SO_3)_2$ salt and Et_4NBF_4 supporting electrolyte. But, ligands **1** and **2** do not react with the supporting electrolyte in the absence of calcium salt. It is noteworthy that the value of the cathodic shift of the oxidation potential of the Fe^{II}/Fe^{III} couple of **1** and **2** upon Ca^{2+} addition (around – 120 mV) is the double of that obtained with the longer disubstituted compound $[Fe(C_5H_4CO-(CH=CH)_2C_6H_4-p–NMe_2)_2]$ (**A**) (−60 mV). This is in agreement with a protonation reaction on the nitrogen atom. Actually, shortening the distance between the redox center and the amino sites increases the electronic communication through the conjugated link. Consequently, upon protonation, the $\Delta E_{1/2}$ value of the Fe oxidation process of ligands **1** and **2** is more important than that of ligand **A**, which is in agreement with the literature data [22]. For all the cited reasons, we propose that the Ca^{2+} electrochemical detection pathway by ligands **1** and **2** involves a protonation reaction due to the presence of the calcium salt, the supporting electrolyte and water traces in the electrochemical medium.

In contrast, the Ba^{2+} electrochemical detection by ligands **1** and **2** is based on a phenomenon very different from that observed in the case of calcium. The variations induced by the presence of the Ba^{2+} cation are not common: the oxidation potential of Fe^{II}/Fe^{III} couple remains roughly the same, while the first oxidation potential of the organic part increases. For classical electrochemical ferrocenyl cation sensors, the intensity of the wave corresponding to the latter oxidation potential generally decreases upon salt addition, or this wave disappears [23]. Most of the time, this oxidation process is also situated after that of the ferrocene unit. An important fact is that no additional wave corresponding to the reduction of NH^+ function was detected here with the barium salt even in excess (50 equiv).

Following the same procedure as for the calcium salt, we decided to prepare CD_3CN mixtures incorporating the ligands (**1** or **2**), the barium salt, and the $^nBu_4NBF_4$ supporting electrolyte in different ratio. In these experiments, we have never detected the formation of the corresponding protonated compounds. Consequently, we propose that, in the case of barium, the electrochemical observations correspond to an averaged phenomenon directly related to the sum of the different metal–ligand interactions. Under our electrochemical conditions, globally, all these interactions are not strong enough to induce a perceptible perturbation of the electron density of the ferrocene unit. The fact that two possible interacting sites compete in the case of ligand **2** probably contributes to weaken the Ba^{2+}–**2** interactions under the electrochemical conditions, inducing thus a weak averaged shift of the oxidation potential of the organic part.

Finally, in the case of zinc and ligand **1**, the explanation of the electrochemical characteristics is not obvious. We suggest that a complex ligand-zinc interaction occurs (as for Ca^{2+} and Ba^{2+}) and competes with a minor protonation reaction. Actually, ^1H NMR spectra of CD_3CN solutions of compound **1** upon Zn^{2+} addition are unclear. In particular, the signals attributed to the phenyl and methyl

groups are very broad, suggesting an interaction with this part of the molecule. Small signals situated around 8.8 ppm could be attributed to NH^+ groups. ^{13}C NMR spectra are not really informative; however, the presence of two small chemical shifts characteristic of the ethyl group of its protonated counterpart **3** was detected.

3. Concluding remarks

In this work, ligands **1** and **2** appear to be good calcium electrochemical sensors. The electrochemical detection pathway of this salt remains the same as that already encountered for their monosubstituted counterparts. These ligands are also "non-classical" barium electrochemical sensors. We show that the pathway of the electrochemical detection of barium is different from that of the calcium. There is no protonation reaction under our electrochemical conditions with barium, and the electrochemical detection is directly related to the ligand–cation interaction. The ligand–cation interactions of these ligands with both salts have been thoroughly studied by NMR and mass spectrometry. These studies highlight the existence of complex equilibriums between different L_nM_m species, all of them being characteristic of the ligand and cation used. In particular the NMR studies show that changing the amino alkyl groups by azacrown rings in the initial framework of **1** enhances the stability of the LM calcium complex. Moreover, this work underlines the fact that the study of the reactivity of electrochemical sensors, as for example the synthesis of compounds **3** and **4**, and of their different ligand–metal interactions, can be useful to clarify the nature of the electrochemical detection phenomena which occur in solution. To our knowledge, this approach is rarely considered in the research field of ion sensing by ferrocenyl ligands.

Finally, with the barium salt, we give evidence for a new and original example of cation electrochemical sensing by ferrocenyl chalcones. Actually, the significant shift of the first oxidation potential of the organic moiety that is observed here in the presence of barium had never been reported beforehand for this class of compounds. As it will soon be highlighted by optical studies, ligands **1** and **2**, and some of their derivatives constitute intriguing examples of multi-channel ion chemosensors.

4. Experimental

4.1. Materials

Toluene, THF and ether were distilled over sodium/benzophenone; pentane, dichloromethane and CH_3CN (pure SDS) were distilled over CaH_2 and stored under argon. EtOH analytical grade (purex SDS) was simply degassed. $Fe(C_5H_4COMe)_2$ (95%, Aldrich), $CHOC_6H_4NEt_2$ (99%, Fluka), $[C_6H_5-p–aza-15-crown-5]$ (98%, Acros), and HBF_4 (54% in Et_2O; Aldrich), $Ca(CF_3SO_3)_2$ (96%, Strem) were used as received. Other salts: $NaCF_3SO_3$ (97%)

$Ba(CF_3SO_3)_2$ (97%) (Fluka), $Zn(CF_3SO_3)_2$ (98%) (Aldrich), $Mg(CF_3SO_3)_2$ (98%) (Fluka). All these salts were dried under vacuum, weighted and added to solution under an argon atmosphere. $[CHOC_6H_4-p–aza-15-crown-5]$ was prepared according to a published procedure [24].

4.2. General instrumentation and procedures

All syntheses were performed under a nitrogen atmosphere using standard Schlenk tube techniques. The solutions of compounds **1** and **2** were light-protected before each measurement. IR spectra were recorded on a Perkin Elmer GX FT-IR spectrophotometer. Samples were run as KBr pellets. Elemental analyses were carried out on a Perkin–Elmer 2400 B analyser at the L. C. C. Microanalytical Laboratory in Toulouse. Mass spectra were obtained at the Service Commun de Spectrométrie de Masse de l'Université Paul Sabatier et du CNRS de Toulouse. Fast atom bombardment (FAB > 0) spectra were performed on a Nermag R 10-10H spectrometer. A 9 kV xenon atom beam was used to desorb samples from the 3-nitrobenzyl alcohol matrix. Other spectra were performed on a triple quadrupole mass spectrometer (Perkin-Elmer Sciex API 365) using electrospray as the ionization mode. The infusion rate was 5 μL/min. ^1H and ^{13}C NMR spectra were performed on Bruker, AM 250, DPX 300 and AMX 400 spectrometers. ^1H and ^{13}C NMR spectra are referenced to external tetramethylsilane. For 2 D NMR experiments, the observation frequencies were in the range of 400.13 MHz for ^1H and 100.62 MHz for ^{13}C in CD_3CN at 293 K.

4.3. Electrochemical studies

Voltammetric measurements were carried out with a home-made potentiostat [25] using the interrupt method to minimize the uncompensated resistance (iR drop). Experiments were performed at room temperature in an airtight three-electrode cell connected to a vacuum/argon line. The reference electrode consisted of a saturated calomel electrode (SCE) separated from the solution by a bridge compartment filled with the same solvent and supporting electrolyte solution. The counter electrode was a platinum wire of ca. 1 cm^2 apparent surface. The working electrode was a Pt electrode (1 mm diameter). The supporting electrolyte ^{n}Bu$_4$NBF$_4$ (99%) (Fluka electrochemical grade) was melted and dried under vacuum for one hour. All solutions measured were 1.0×10^{-3} M in organometallic complex and 0.1 M in supporting electrolyte. The solutions were degassed by bubbling argon before experiments. With the above reference, $E_{1/2} = 0.45$ V vs. SCE was obtained for 1 mM ferrocene (estimated experimental uncertainty of ±10 mV). Cyclic voltammetry was performed in the potential range −2 to 2 V vs. SCE scanning from 0 to 2 V/SCE for oxidation studies (and from 0 to −2 V/SCE for reduction studies) at 0.1 V s^{-1}, at room temperature. Before each measurement, the electrode was

polished with Emery paper (Norton A621). To calculate the half wave potential ($E_{1/2}$), a quasi-steady state behaviour (at Pt working electrode: 1 mm of diameter) is obtained by the use of linear voltammetry at 5 mV s^{-1}. For cation detection experiments, concentrated acetonitrile solutions of calcium triflate (0.3–10 equiv) were syringed into the ferrocenyl solution under argon atmosphere, keeping the total volume of the electrochemical mixture constant. The solution was immediately degassed and examined.

4.4. Proton NMR titration studies

Proton NMR titrations were typically performed as followed. A solution (500 μL) of receptors **1–2** in a deuterated solvent was added (using a microsyringe) into NMR tubes containing the appropriate quantities of solid Ca(CF$_3$SO$_3$)$_2$ salt under inert atmosphere. The NMR spectrum of the receptor alone and of each mixture was monitored. The samples of solid calcium were prepared by evaporating the corresponding calculated volumes of a calcium guest solution (10^{-2} M) in acetonitrile. Stability constants were evaluated from titration data using the method indicated in the main text.

4.5. [Fe(C$_5$H$_4$COCH═CHC$_6$H$_4$NEt$_2$)$_2$] (1)

A light-protected mixture of Fe(C$_5$H$_4$COMe)$_2$ 0.250 g (0.93 × 10^{-3} mol), CHOC$_6$H$_4$NEt$_2$ 0.328 g (1.85 × 10^{-3} mol), and 1 equiv of NaOH was dissolved in ethanol (20 mL) and stirred for 4 h at room temperature. The mixture was evaporated to dryness. The residue was purified by column chromatography on dried silica (eluent: 2.5:0.4 toluene/ethyl acetate) and the red phase obtained was extracted with THF as eluent (thrice). After evaporation of the solvent, the product was washed with pentane (30 mL × 2) and dried to afford the desired product as a deep orange powder in 60% yield ($m = 0.327$ g). NMR ^{1}H: δ 1.19 (t, 12H, $^3J_{HpHq} = 7.1$ Hz, Hq), 3.45 (q, 8H, $^3J_{HpHq} = 7.1$ Hz, Hp), 4.59 (m, 4H, $^3J_{HeHf} = 1.9$ Hz, Hf), 4.91 (m, 4H, $^3J_{HeHf} = 1.9$ Hz, He), 6.70 (d, 4H, $^3J_{HcHd} = 9$ Hz, Hd), 7.01 (d, 2H, $^3J_{HbHa} = 15.4$ Hz, Ha), 7.57 (d, 4H, $^3J_{HcHd} = 9.0$ Hz, Hc), 7.60 (d, 2H, $^3J_{HaHb} = 15.4$ Hz, Hb). ^{13}C {^{1}H} NMR: δ 12.29 (CHq), 44.52 (CHp), 71.28 (CHe), 73.83 (CHf), 83.41 (Cipso-C$_5$H$_4$), 111.60 (CHd), 117.79 (CHa), 122.04 (Cipso-C), 131.06 (CHc), 142.06 (CHb), 150.05 (Cipso-N), 191.61 (CO). IR (CH$_3$CN): 1522, 1552, 1575, 1611, 1647 (v_{CO}), 2873–2975 (v_{CH}). Anal. Calc. for **3**, C$_{36}$H$_{40}$N$_2$O$_2$Fe: C, 73.47; H, 6.85; N, 4.76. Found: C, 73.38; H, 6.91; N, 4.83%.

4.6. [Fe(C$_5$H$_4$COCH═CHC$_6$H$_4$-p–aza-15-crown-5)$_2$] (2)

Same procedure as for **1** with a mixture of [Fe(C$_5$H$_4$COMe)$_2$] 0.148 g (0.55 × 10^{-3} mol), N-(4-formylphenyl)aza-15-crown-5] 0.370 g (1.10 × 10^{-3} mol), and NaOH

0.022 g (0.55 × 10^{-3} mol) in ethanol (15 mL); eluent: 2:1.5 toluene/ethyl acetate. The product is obtained as an orange powder in 62% yield ($m = 0.299$ g). NMR ^{1}H: δ 3.57-3.73 (m, 8H, Hs), 3.59 (m, 8H, Hp), 3.62 (m, 8H, Hr), 3.62 (m, 8H, Ht), 3.73 (m, 8H, Hq), 4.59 (m, 4H, $^3J_{HeHf} = 1.8$ Hz, Hf), 4.91 (m, 4H, He), 6.70 (d, 4H, $^3J_{HcHd} = 8.9$ Hz, Hd), 7.02 (d, 2H, $^3J_{HaHb} = 15.4$ Hz, Ha), 7.57 (d, 4H, $^3J_{HcHd} = 8.9$ Hz, Hc), 7.60 (d, 2H, $^3J_{HaHb} = 15.4$ Hz, Hb). ^{13}C {^{1}H} NMR: δ 52.87 (CHp), 68.48 (CHq), 69.76 (CHt), 70.30 (CHs), 70.96 (CHr), 71.35 (CHe), 73.89 (CHf), 83.38 (Cipso-C$_5$H$_4$), 111.97 (CHd), 118.30 (CHa), 122.78 (Cipso-C), 130.87 (CHc), 141.91 (CHb), 150.08 (Cipso-N), 191.71 (CO). IR (CH$_3$CN): 1521, 1550, 1577, 1611, 1648 (v_{CO}), 2873–3001 ($v_{CH_2-O-CH_2}$). MS (FAB): Anal. Calcd for **2**, C$_{48}$H$_{60}$N$_2$O$_{10}$Fe: C, 65.45; H, 6.87; N, 3.18. Found: C, 65.28; H, 6.93; N, 3.12%.

4.7. [Fe(C$_5$H$_4$COCH═CHC$_6$H$_4$NHEt$_2$)$_2$][BF$_4$]$_2$ (3)

See main text. NMR ^{1}H: δ 1.16 (t, 12H, $^3J_{HpHq} = 7.2$ Hz, Hq), 3.68 (m, 8H, Hp), 4.74 (m, 4H, $^3J_{HeHf} = 2,0$ Hz Hf), 5.02 (m, 4H, $^3J_{HeHf} = 2,0$ Hz, He), 7.30 (d, 2H, $^3J_{HaHb} = 15.7$ Hz, Ha), 7.62 (d, 4H, $^3J_{HcHd} = 8.7$ Hz, Hd), 7.72 (d, 2H, $^3J_{HaHb} = 15.7$ Hz, Hb), 8.01 (d, 4H, $^3J_{HdHc} = 8.7$ Hz, Hc), 9.14 (br s, 2H, NH$^+$). ^{13}C {^{1}H} NMR δ 10.15 (CHq), 54.64 (CHp), 71.76 (CHe), 74.85 (CHf), 82.93 (Cipso-C$_5$H$_4$), 123.39 (CHd), 126.21 (CHa), 130.86 (CHc), 138.00 (Cipso-N), 138.05 (Cipso-C), 138.55 (CHb), 191.55 (CO). MS (FAB): [M−CF$_3$SO$_3$]$^+$ = 739.

4.8. [Fe(C$_5$H$_4$COCH═CHC$_6$H$_4$-p–aza-15-crown-5H)$_2$][BF$_4$]$_2$ (4)

HBF$_4$ · Et$_2$O (2 equiv) was slowly syringed into a stirred solution of **2** 0.050 g (0.06 × 10^{-3} M) in acetonitrile (8 mL). The light-protected mixture solution was stirred for 1 h. After solvent evaporation, the product was washed with ether (30 mL) and pentane (50 mL) and dried under vacuum. A violet powder was obtained in 65% yield ($m = 0.039$ g). NMR ^{1}H: δ 3.10, 3.81 (m, 8H, Hq), 3.37, 3.72 (m, 8H, Hr), 3.66 (m, 8H, Hs), 3.77 (m, 8H, Ht), 3.93 (m, 8H, Hp), 4.73 (m, 4H, $^3J_{HeHf} = 2.0$ Hz, Hf), 5.01 (m, 4H, $^3J_{HeHf} = 2.0$ Hz, He), 7.34 (d, 2H, $^3J_{HaHb} = 15.7$ Hz, Ha), 7.74 (d, 2H, $^3J_{HaHb} = 15.4$ Hz, Hb), 7.95 (d, 4H, $^3J_{HcHd} = 8.8$ Hz, Hd), 8.04 (d, 4H, $^3J_{HcHd} = 8.8$ Hz, Hc), 8.52 (br s, 2H, NH$^+$). ^{13}C {^{1}H} NMR: δ 58.77 (CHp), 63.15 (CHq), 68.90 (CHs), 69.00 (CHt), 70.76 (CHr), 71.76 (CHe), 74.92 (CHf), 82.40 (Cipso-C$_5$H$_4$), 124.31 (CHd), 126.23 (CHa), 130.65 (CHc), 136.35 (Cipso-N), 138.39 (Cipso-C), 138.68 (CHb), 191.67 (CO). IR (KBr): 1515, 1594, 1605, 1654 (v_{CO}), 2876–2921 ($v_{CH_2-O-CH_2}$), 3050–3152 (vNH$^+$). ES-MS: [M−BF$_4$]$^+$ = 969.7. Anal. Calc. for **2**, C$_{48}$H$_{62}$N$_2$O$_{10}$FeB$_2$F$_8$: C, 54.57; H, 5.91; N, 2.65. Found: C, 54.38; H, 5.93; N, 2.52%.

4.9. Interaction of compound *1* with 2 equiv of Ca(CF₃SO₃)₂

NMR ^{1}H: δ 1.15 (t, 12H, $^3J_{p-q}$ = 7,1 Hz, Hq), 3.42 (q, 8H, $^3J_{q-p}$ = 7.1 Hz, Hp), 4.80 (br s, 4H, Hf), 5,07 (br s, 4H, He), 6.59 (d, 4H, $^3J_{c-d}$ = 8.4 Hz, Hd), 6.93 (d, 2H, $^3J_{b-a}$ = 15.2 Hz, Ha), 7.48 (d, 4H, $^3J_{d-c}$ = 8,4 Hz, Hc), 7,92 (d, 2H, $^3J_{a-b}$ = 15.2 Hz, Hb). NMR ^{13}C {^{1}H}: δ 11.67 (CHq), 44.67 (CHp), 72.93 (CHe), 75.11 (CHf), 82.76 (Cipso-C₅H₄), 111.61 (CHd), 115.47 (CHa), 121.37 (Cipso-C), 132.48 (CHc), 148.35 (CHb), 151.09 (Cipso-N), 194.87 (CO), 121.04 (q, $^1J_{C-F}$ = 320 Hz, CF₃SO₃).

4.10. Interaction of compound *2* with 2 equiv of Ca(CF₃SO₃)₂

NMR ^{1}H: δ 3.54 (t, 8H, $^3J_{HqHp}$ = 5.6 Hz, Hp), 3.52–3.91 (m, 24H, Hr, Hs, Ht), 3.88 (t, 8H, $^3J_{HqHp}$ = 5.6 Hz, Hq), 4.73 (m, 4H, $^3J_{HeHf}$ = 2.0 Hz, Hf), 4.99 (m, 4H, $^3J_{HeHf}$ = 2.0 Hz, He), 7.08 (d, 2H, $^3J_{HaHb}$ = 15.6 Hz, Ha), 7.16 (br d, 4H, $^3J_{HcHd}$ = 8.4 Hz, Hd), 7.70 (d, 4H, $^3J_{HcHd}$ = 8.4 Hz, Hc), 7.72 (d, 2H, $^3J_{HaHb}$ = 15.6 Hz, Hb). ^{13}C {^{1}H} NMR: δ 53.03 (CHp), 68.93 (CHq), 68.98, 69.90, 70.11 (CHr, CHs, CHt), 72.11 (CHe), 74.77 (CHf), 82.76 (Cipso-C₅H₄), 118.81 (CHd), 121.03 (CHa), 128.11 (Cipso-C), 130.65 (CHc), 142.81 (CHb), 151.57 (Cipso-N), 192.96 (CO).

Acknowledgement

References

[1] (a) For examples: W.-J. Zhou, S.-J. Ji, Z.-L. Shen, J. Organomet. Chem. 691 (2006) 1356–1360;
(b) Z.-L. Shen, S.-J. Ji, W.-J. Zhou, Synth. Commun. 35 (2005) 1903–1909;
(c) M. Sun, Q. Shi, G. Huang, Y. Liang, Y. Ma, Synthesis 15 (2005) 2482–2486;
(d) Z.-L. Shen, D.-G. Gu, S.Y. Wang, J. Organomet. Chem. 689 (2004) 1843–1848;
(e) M. Prokesova, E. Solcaniova, S. Toma, K.W. Muir, A.A. Torabi, G. Knox, J. Org. Chem. 61 (1996) 3392–3397;
(f) D. Villemin, B. Martin, M. Puciova, S. Toma, J. Organomet. Chem. 484 (1994) 27–31;
(g) A.G. Nagy, P. Sohar, J. Marton, J. Organomet. Chem. 410 (1991) 357–364;
(h) A.G. Nagy, J. Organomet. Chem. 291 (1985) 335–340;
(i) A.G. Nagy, S. Toma, J. Organomet. Chem. 266 (1984) 257–268;
(j) A.M. El-Khawaga, K.M. Hassan, A.A. Khalaf, Z. Naturforsch. 36b (1981) 119–122;
(k) A.N. Nesmeyanov, G.B. Shulp'in, L.V. Rybin, N.T. Gubenko, M.I. Rybinskaya, P.V. Petrovkii, V.I. Robas, J. Gen. Chem. USSR 44 (1974) 1994–2001;
(l) S. Stankovianski, A. Beno, S. Toma, E. Gono, Chem. Zvesti 24 (1970) 19–27;
(m) S. Toma, A. Perjessy, Chem. Zvesti 23 (1969) 343–351;
(n) J.P.C.G. Dubosc, U.S. Patent 3, 1967, 335,008;
(o) M. Furdik, S. Toma, Chem. Zvesti 20 (1966) 326–335;
(p) J. Boichard, J.P. Monin, J. Tirouflet, Bull. Soc. Chim. Fr. 4 (1963) 851–856;
(q) T.A. Mashburn Jr., C.E. Cain, C.R. Hauser, J. Org. Chem. 25 (1960) 1982–1986.
[2] (a) X. Wu, E.R.T. Tieking, I. Kostetski, N. Kocherginsky, A.L.C. Tan, S.B. Khoo, P. Vilairat, M.-L. Go, Eur. J. Pharm. Sci. 27 (2006) 175–187;
(b) Q.-B. Song, X.-N. Li, T.-H. Shen, S.-D. Yang, G.-R. Qiang, X.-L. Wu, Y.-X. Ma, Synth. Commun. 33 (2003) 3935–3941;
(c) X. Wu, P. Wilairat, M.-L. Go, Bioorg. Med. Chem. Lett. 12 (2002) 2299–2302;
(d) A. Ferle-Vidovic, M. Poljak-Blazi, V. Rapic, D. Skare, Cancer Biother. Radiopharm. 15 (2000) 617–624.
[3] (a) F. Sancenon, A. Benito, F.J. Hernandez, J.M. Lloris, R. Martinez-Manez, T. Pardo, R. Soto, Eur. J. Inorg. Chem. (2002) 866–875;
(b) S. Fery-Forgues, B. Delavaux-Nicot, J. Photochem. Photobiol. A Chem. 132 (2000) 137–159;
(c) B. Delavaux-Nicot, S. Fery-Forgues, Eur. J. Inorg. Chem. (1999) 1821–1825;
(d) P.D. Beer, F. Szemes, V. Balzani, C.M. Salà, M.G.B. Drew, S.W. Dent, M. Maestri, J. Am. Chem. Soc. 119 (1997) 11864–11875;
(e) P.D. Beer, A.R. Graydon, L.R. Sutton, Polyhedron 15 (1996) 2457–2461.
[4] (a) F. Sancenon, A. Benito, F.J. Hernandez, J.M. Lloris, R. Martinez-Manez, T. Pardo, J. Soto, Eur. J. Inorg. Chem. (2002) 866–875;
(b) F. Oton, A. Tarraga, M.D. Velasco, A. Espinosa, P. Molina, Chem. Commun. (2004) 1658–1659;
(c) L.-J. Kuo, J.-H. Liao, C.-T. Chen, C.-H. Huang, C.-H. Chen, J.-M. Fang, Org. Lett. 5 (2003) 1821–1824.
[5] J. Maynadié, B. Delavaux-Nicot, D. Lavabre, B. Donnadieu, J.C. Daran, A. Sournia- Saquet, Inorg. Chem. 43 (2004) 2064–2077.
[6] B. Delavaux-Nicot, J. Maynadié, D. Lavabre, C. Lepetit, B. Donnadieu, Eur. J. Inorg. Chem. (2005) 2493–2505.
[7] J. Maynadié, B. Delavaux-Nicot, D. Lavabre, S. Fery-Forgues, J. Organomet. Chem. 691 (2006) 1101–1109.
[8] J. Maynadié, B. Delavaux-Nicot, S. Fery-Forgues, D. Lavabre, R. Mathieu, Inorg. Chem. 41 (2002) 5002–5004.
[9] B. Delavaux-Nicot, J. Maynadié, D. Lavabre, S. Fery-Forgues, Inorg. Chem. 45 (2006) 5691–5702.
[10] K. Rurack, J.L. Bricks, G. Reck, R. Radeglia, U. Resh-Genger, J. Phys. Chem. A. 104 (2000) 3087–3109.
[11] (a) P.D. Beer, C. Blackburn, J.F. McAleer, H. Sikaniaka, Inorg. Chem. 29 (1990) 378–381;
(b) M. Spescha, N.W. Duffy, B.H. Robinson, J. Simpson, Organometallics 13 (1994) 4895–4904;
(c) N.W. Duffy, J. Harper, P. Ramani, R. Ranatunge-Bandarage, B.H. Robinson, J. Simpson, J. Organomet. Chem. 564 (1998) 125–131.
[12] (a) P.D. Beer, J. Cadman, Coord. Chem. Rev. 205 (2000) 131–155;
(b) P.D. Beer, M.G.B. Drew, J. Pilgrim, Inorg. Chim. Acta 225 (1994) 137–144.
[13] (a) M.J. Hynes, J. Chem. Soc. Dalton Trans. (1993) 311–312;
(b) L. Fielding, Tetrahedron 56 (2000) 6151–6170.
[14] (a) N. Marcotte, S. Fery-Forgues, D. Lavabre, S. Marguet, V.G. Pivovarenko, J. Phys. Chem. A 103 (1999) 3163–3170;
(b) S. Fery-Forgues, D. Lavabre, D. Rochal, New J. Chem. 22 (1998) 1531–1538.
[15] (a) C.J. Pedersen, H.K. Frendsdorff, Angew. Chem. Int., Ed. Engl. 11 (1972) 16–25;
(b) B.J. Dietrich, J. Chem. Educ. 62 (1985) 954–964.
[16] (a) P.D. Beer, A.D. Keefe, H. Sikanyika, C. Blackburn, J.M. McAleer, J. Chem. Soc. Dalton. Trans. (1990) 3289–3294;
(b) P.D. Beer, H. Sikanyika, A.M.Z. Slavin, D.J. Williams, Polyhedron 8 (1989) 879–886;
(c) T. Akutagawa, N. Takamatsu, K. Shitagami, T. Hasegawa, T. Nakamura, T. Inabe, W. Fujita, K. Awaga, J. Mater. Chem. 11 (2001) 2118–2124;

(d) J. Otsuki, T. Yamagata, K. Ohmuro, K. Arabi, T. Takido, M. Seno, Bull. Chem. Soc. Jpn. 74 (2001) 333.

[17] (a) S. Itoh, H. Kumey, S. Nagatomo, T. Kitagawa, S. Fukuzumi, J. Am. Chem. Soc. 123 (2001) 2165–2175;
(b) D. Hall, A. Leineweber, J.H.R. Tucker, D. Williams, J. Organomet. Chem. 523 (1996) 13–22;
(c) J. Hu, L.J. Barbour, R. Ferdani, G.W. Gokel, J. Chem. Commun. (2002) 1806–1807.

[18] (a) G.A. Lawrance, Chem. Rev. 86 (1986) 17–33;
(b) A.D. Frankland, P.B. Hitchcok, M.F. Lappert, G.A. Lawless, J. Chem. Soc., Chem. Commun. (1994) 2435–2436;
(c) A. Onoda, Y. Yamada, M. Doi, T. Okamura, N. Ueyama, Inorg. Chem. 40 (2001) 516–521.

[19] (a) G.W. Gokel, S.L. De Wall, E.S. Meadous, Eur. J. Org. Chem. (2000) 2967–2978;

(b) E.S. Meadous, S.L. De Wall, L.J. Barbour, G.W. Gokel, J. Am. Chem. Soc. 123 (2001) 3092–3107;
(c) J.C. Ma, D.A. Dougherty, Chem. Rev. (1997) 1303–1324;
(d) T. Futterer, A. Merz, J. Lex, Angew. Chem., Int. Ed. Engl. 36 (1997) 611–613.

[20] R.C. Weast (Ed.), Handbook of Chemistry and Physics, 65th ed., CRC Press, Boca Raton, FL, 1985.

[21] F. Vögtle, Supramolecular Chemistry, Wiley, New York, 1991.

[22] H. Plenio, J. Yang, R. Diodone, J. Heinze, Inorg. Chem. 33 (1994) 4098–4104.

[23] M.P. Andrews, C. Blackburn, J.F. McAleer, V.D. Patel, J. Chem. Soc., Chem. Commun. (1987) 1122–1124.

[24] J.P. Dix, F. Vögtle, Chem. Ber. 113 (1980) 457–470.

[25] P. Cassoux, R. Dartiguepeyron, D. de Montauzon, J.B. Tommasino, P.L. Fabre, Actual. Chim. 1 (1994) 49–55.